Biophysical Journal Volume 104 June 2013 2662–2670

An Embryonic Myosin Isoform Enables Stretch Activation and Cyclical Power in *Drosophila* Jump Muscle

Cuiping Zhao and Douglas M. Swank*
Department of Biology and Center for Biotechnology and Interdisciplinary Studies, Rensselaer Polytechnic Institute, Troy, New York

ABSTRACT The mechanism behind stretch activation (SA), a mechanical property that increases muscle force and oscillatory power generation, is not known. We used *Drosophila* transgenic techniques and our new muscle preparation, the jump muscle, to determine if myosin heavy chain isoforms influence the magnitude and rate of SA force generation. We found that *Drosophila* jump muscles show very low SA force and cannot produce positive power under oscillatory conditions at pCa 5.0. However, we transformed the jump muscle to be moderately stretch-activatable by replacing its myosin isoform with an embryonic isoform (EMB). Expressing EMB, jump muscle SA force increased by 163% and it generated net positive power. The rate of SA force development decreased by 58% with EMB expression. Power generation is Pi dependent as >4 mM Pi was required for positive power from EMB. Pi increased EMB SA force, but not wild-type SA force. Our data suggest that when muscle expressing EMB is stretched, EMB is more easily driven backward to a weakly bound state than wild-type jump muscle. This increases the number of myosin heads available to rapidly bind to actin and contribute to SA force generation. We conclude that myosin heavy chain isoforms influence both SA kinetics and SA force, which can determine if a muscle is capable of generating oscillatory power at a fixed calcium concentration.

INTRODUCTION

Stretch activation (SA) is a delayed force increase following a rapid stretch of a calcium-activated muscle fiber (Fig. 1). SA force generation is most prominent in asynchronous insect flight muscle, moderate in heart muscle, and least prominent in vertebrate skeletal muscle (1,2). For muscles that undergo oscillatory contractions (cyclical lengthening and shortening), prominent SA increases force during the shortening portion of the cycle so that it is greater than force during lengthening (3). This enables or enhances the muscle's ability to produce power. For insect flight muscles, SA enables positive work and power generation without the need for calcium release and uptake during each contraction cycle (2). In the heart, SA increases contractility in response to increased filling, and hence increases cardiac output (4). Conversely, most vertebrate skeletal muscles only display very small and transient SA, and their muscle contraction and force levels are almost solely dependent on intracellular calcium concentration (1).

Due to its physiological importance in insect and cardiac muscle, SA has been studied for ~30 years. However, the underlying mechanism is still unknown. By using mechanical, ultrastructural, and genetic techniques, several mechanisms have been proposed by researchers including the thick and thin filament lattice-matching model (5), stretching of connecting filaments running between the Z-bands and thick filaments increasing cross-bridge binding probability (6,7), phosphorylation of the myosin regulatory light chain increasing cross-bridge force generation (8,9), myosin-troponin bridges relieving tropomyosin's blocking of actin binding sites (10,11), and strain-induced alterations in myosin isoform kinetics (12). Myosin heavy chain (MHC) isoforms found in different muscle types have been previously studied for effects on SA, but almost all studies have focused on their ability to modify the kinetics of SA, the rate of force regeneration (13–15), rather than the magnitude of SA force generation (F_{SA}).

Drosophila is an excellent experimental model for examining myosin's role in SA because all *Drosophila* muscle MHC isoforms are encoded by a single *Mhc* gene, and the existence of muscle-specific myosin null lines (16,17). This enables different myosin isoforms and mutants to be expressed in various muscle types through relatively simple transgenic manipulations (18). The ability to isolate and mechanically evaluate two major muscle types from the *Drosophila* thorax, the indirect flight muscle (IFM) and the jump muscle (tergal depressor of the trochanter), is another advantage of this model system (19). The *Drosophila* jump muscle powers fly jumping and contributes to flight initiation (20,21). Jump muscle activation is thought to depend primarily on intracellular calcium concentration rather than SA (22).

To explore the molecular basis behind SA, we used *Drosophila* to perform a potential gain of function study of MHC effects on SA properties by replacing the native jump muscle myosin with an embryonic myosin isoform (EMB). We found that skinned jump muscle has minimal F_{SA} and cannot generate positive power in an oscillatory manner when calcium activated. However, when we transgenically replaced the endogenous jump muscle myosin with EMB, it transformed the jump muscle into a moderately stretch-activatable muscle type and enabled it to generate power under sinusoidal length change conditions.

Submitted January 14, 2013, and accepted for publication April 29, 2013.
*Correspondence: swankd@rpi.edu
Editor: Christopher Berger.
© 2013 by the Biophysical Society
0006-3495/13/06/2662/9 $2.00
http://dx.doi.org/10.1016/j.bpj.2013.04.057

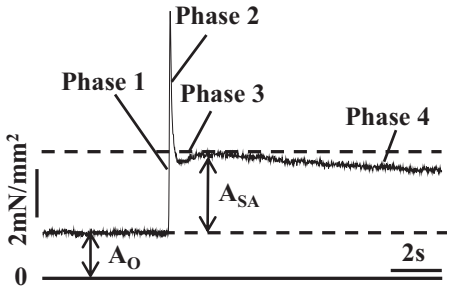

FIGURE 1 Representative example of a stretch activation trace in response to a 1% ML increase over 0.5 ms from a control *Drosophila* jump muscle fiber at pCa 5.0. A_{SA} is total stretch-activated force and A_O is total calcium-activated isometric force. Baseline is 0 tension. Phases are labeled according to Huxley and Simmon's model (25). Phase 3 is SA.

This shows that MHC isoforms can significantly influence not just SA kinetics, but also F_{SA}. In addition, we found that EMB F_{SA} and power output is Pi concentration dependent. The response of EMB to Pi suggests that the mechanism for increasing SA by myosin isoforms likely involves cross-bridge steps associated with Pi release and rebinding. We propose a mechanism based on muscle expressing EMB myosin being more responsive to stretch and/or stretch increasing EMB's affinity for Pi more than jump muscle myosin.

MATERIALS AND METHODS

Transgenic *Drosophila* lines

The control fly line is the wild-type myosin transgene, *pwMhc*2, expressed in a *Drosophila* line null for myosin in the jump and indirect flight muscles, Mhc^{10}. Details of its creation are described in Swank et al. (18). The transgene expresses the native myosin isoform normally found in each fiber type. Creation of the EMB transgenic *Drosophila* line is described in Wells et al. (23). This line expresses an embryonic cDNA transgenic construct behind the myosin promoter. When crossed with the myosin null line, Mhc^{10}, it expresses only the EMB myosin isoform in the jump muscle. Expression of EMB does not alter jump muscle ultrastructure (23), and the flies are still able to jump (24). All transgenic fly lines were maintained at 25°C on a 12-h light-dark regiment.

Jump muscle preparation

Dissection and mounting of jump muscle fibers for mechanical evaluation were performed as previously described (24). Briefly, jump muscle fibers were removed from the thorax of 2–3-day-old female *Drosophila* and chemically demembranated in dissection solution (pCa 8.0, 5 mM MgATP, 1 mM free Mg^{2+}, 0.25 mM phosphate, 5 mM EGTA, 20 mM N,N-Bis(2-hydroxyethyl)-2-aminoethanesulfonic acid (BES, pH 7.0), adjusted to 175 mM ionic strength with Na methane sulfonate, 1 mM DTT, 50% glycerol, and 0.5% Triton X-100) for 1 h at 4°C. The isolated jump muscle fibers were secured with aluminum T-clips at both ends and mounted on a mechanics rig with one end connected to a force gauge and the other end connected to a servo motor (19).

The fibers were stretched in relaxing solution (pCa 8.0, 10 mM MgATP, 0 mM phosphate, 45 mM creatine phosphate, 450 units/ml creatine phosphokinase, 1 mM free Mg^{2+}, 5 mM EGTA, 20 mM pH7.0 BES, 260 mM ionic strength, adjusted with Na methane sulfonate, 1 mM DTT) until the optimal sarcomere length, 3.6 μm, was reached (24). Fiber dimensions were measured at this length. Preactivation solution (EGTA decreased to 0.5 mM) was exchanged for relaxing solution to help maintain sarcomere homogeneity during activation. Activating solution (pCa 5.0, 20 mM MgATP, 0, 8 or 16 mM phosphate, 25 mM creatine phosphate, 450 units/ml creatine phosphokinase, 1 mM free Mg^{2+}, 5 mM EGTA, 20 mM pH7.0 BES, adjusted to 260 mM ionic strength with Na methane sulfonate, 1 mM DTT) was exchanged into the bathing chamber to activate fibers to pCa 5.0. The ingredients of our solutions necessitated an ionic strength of 260 mM to allow for high ATP, creatine phosphate, and phosphate concentrations. High ATP and creatine phosphate are needed as our previous study showed *Drosophila* myosins have unusually low ATP affinity (19). Mechanical measurements (step analysis, sinusoidal analysis, and work loop analysis) were performed at optimal sarcomere length at 15°C. Isometric tension was monitored throughout the mechanics experiments.

Muscle mechanics protocols

Isometric tension

Total isometric tension (A_O) of skinned jump muscle fibers expressing the native (control) and EMB myosin isoforms was measured in our activating solutions containing 0, 8, or 16 mM Pi at pCa 5.0 at a sarcomere length of 3.6 μm. A_O is composed of two components, passive (relaxed) tension (R_O), measured in our relaxing solution at pCa 8.0, and calcium-activated tension (F_O). F_O was obtained by subtracting R_O from A_O ($F_O = A_O - R_O$). Fibers producing an initial isometric tension <15 mN/mm^2 at a starting concentration of 0 mM Pi or <10 mN/mm^2 at a starting concentration of 16 mM Pi were discarded. Half the experiments were started at 16 mM Pi and the other half at 0 mM to control for possible effects of fiber degradation during the experiment.

Step analysis

Step analysis was performed in activation solution (pCa 5.0) at 0, 8, and 16 mM Pi to measure the SA response of jump muscle fibers. For each [Pi], a lengthening step of 1% muscle length (ML) over 0.5 ms was applied and the corresponding tension response was recorded. The length step was held for 300 ms and fibers were slowly returned to their original length over 500 ms. Isometric tension was measured before and after each length step to monitor the condition of the muscle. If the muscle deteriorated significantly, >10% of the previous isometric force, the muscle was discarded. The total SA magnitude (A_{SA}) was measured by subtracting the total Ca^{2+}-activated isometric tension (A_O) from the peak value of phase 3 (Fig. 1). Passive SA tension (R_{SA}), obtained from length steps in relaxation solution (pCa 8.0), was used to calculate stretch-activated tension, $F_{SA} = A_{SA}$-R_{SA}.

The rate of SA (r_3, rate constant of phase three) and the rates of phase two, r_2, and four, r_4, were obtained by fitting the tension transient following the initial spike, Huxley and Simmon's phases two through four (25), to the sum of 3 exponential curves: $a_3[1\text{-}\exp(-r_3t)] + a_2\exp(-r_2t) + a_4\exp(-r_4t) +$ offset (Fig. 1).

Work loops

The work loop assay was performed to measure muscle power output under high strain amplitudes at 0, 8, and 16 mM Pi (19). Fibers were oscillated through a sinusoidal waveform at various frequencies (1–60 Hz) and strain amplitudes (0.25–1% ML) to find the conditions that produced maximum power. Ten identical consecutive cycles of sinusoidal waveforms were applied to the fibers. Both tension and ML traces were recorded at a sampling rate of 8 Hz. Work was determined by integrating the area under the tension-length curve during oscillation, and power calculated by multiplying the net work by oscillation frequency (19). We used the work and power values from the eighth cycle where fibers reached a plateau for power production.

Sinusoidal analysis

Sinusoidal analysis was performed to determine muscle power generation and muscle stiffness characteristics under low strain amplitudes, 0.25% peak to peak, over a range of frequencies, 0.5–500 Hz as previously described (19,26). Fibers were subjected to 0, 8, and 16 mM Pi concentrations.

RESULTS

Isometric tension

Drosophila jump muscle Ca^{2+}-activated isometric tension increased when the native myosin was replaced with the EMB isoform (Table 1). A_O and F_O were 72% higher compared to control fibers. R_O values were low for both control and EMB fibers, ~13% of A_O, and were not significantly different.

Stretch activation magnitude

Our skinned, control *Drosophila* jump muscles displayed the classic components of a length step response. The response consisted of an immediate tension increase (phase 1), a quick tension drop (phase 2), a delayed secondary tension increase (phase 3), and a slow tension recovery (phase 4) following a 1% fiber stretch over 0.5 ms (Fig. 1). Phase 3 of the tension transient is SA. Stretch-activated tension (F_{SA}) of control fibers was 2.6 ± 0.5 mN/mm^2. This is only a 12% increase above F_O, showing that the muscle is only minimally stretch-activated (Table 2). R_{SA} accounted for 32% of A_{SA} (Table 2).

The EMB myosin isoform transformed the jump muscle into a moderately stretch-activated muscle as F_{SA} was 163% greater than control fibers at 8 mM Pi (Fig. 2, *A* and *B*). To determine if the increase in F_{SA} from EMB expression is due to EMB's general ability to produce higher forces, as its isometric tension was higher than control fibers (Table 2), F_{SA} was normalized to F_O. The normalized SA magnitude (F_{SA}/F_O) of EMB fibers was still higher, 67%, compared to control fibers under the same experimental conditions (8 mM Pi) (Fig. 2 *C* and Table 2).

Kinetics of stretch activation

Expressing the EMB isoform decreased the rate of stretch activation, r_3, of jump muscle fibers by 58% (Fig. 3). The rate of phase 2 decreased by about the same amount, 56%, as phase 3, but the rate of phase 4 was not changed (Table 3).

TABLE 1 Isometric tension of *Drosophila* jump muscles

	A_O (mN/mm^2)	R_O (mN/mm^2)	F_O (mN/mm^2)	*n*
Control	24.9 ± 2.1	3.2 ± 0.8	21.8 ± 2.2	10
EMB	42.8 ± 3.8[a]	5.4 ± 1.7	37.4 ± 4.2[a]	11

Values are mean ± SE; *n*, number of fibers; A_O, total isometric tension measured at pCa 5.0, 8 mM Pi, 15°C. R_O, passive tension measured at pCa 8.0, 8 mM Pi. F_O, net active isometric tension after subtracting passive tension ($F_O = A_O$-R_O).
[a]$P < 0.05$, significantly different from control, Student's *t-test*.

TABLE 2 SA magnitude of *Drosophila* jump muscle fibers

	A_{SA} (mN/mm^2)	R_{SA} (mN/mm^2)	F_{SA}(mN/mm^2)	F_{SA}/Fo	*n*
Control	3.8 ± 0.4	1.2 ± 0.3	2.6 ± 0.5	0.12 ± 0.02	10
EMB	8.8 ± 0.8[a]	2.0 ± 0.6	6.8 ± 1.0[a]	0.20 ± 0.03[a]	16

Values are mean ± SE; *n*, number of fibers. A_{SA} total stretch-activated tension measured at pCa 5.0, 8 mM Pi, R_{SA} passive elastic component of stretch-activated tension measured at pCa 8.0, F_{SA} net stretch-activated tension ($F_{SA} = A_{SA}$-R_{SA}).
[a]$P < 0.05$, significantly different from control, Student's *t-test*.

Power generation

Work loop analysis

We measured the capability of *Drosophila* jump muscles to produce power under optimized cyclical conditions at 8 mM

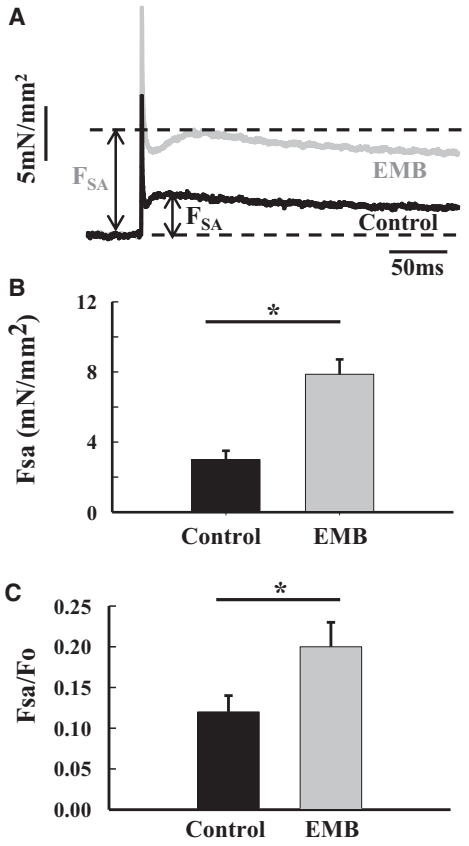

FIGURE 2 Comparison of stretch activation magnitude between EMB and control jump muscle fibers at 8 mM Pi. (*A*) Individual stretch activation traces following a 1% ML step over 0.5 ms from control and EMB fibers. (*B*) F_{SA} of EMB fibers increased by 163% compared to control fibers (*$P < 0.05$, Student's *t-test*). Note that a passive tension trace collected at pCa 8.0 was subtracted from each trace. Thus, the traces shown are only from active muscle processes. (*C*) EMB F_{SA}, normalized to F_O, increased 67% compared to control jump muscle fibers (*$P < 0.05$, Student's *t-test*). F_{SA} is stretch-activated force and F_O is calcium-activated isometric force.

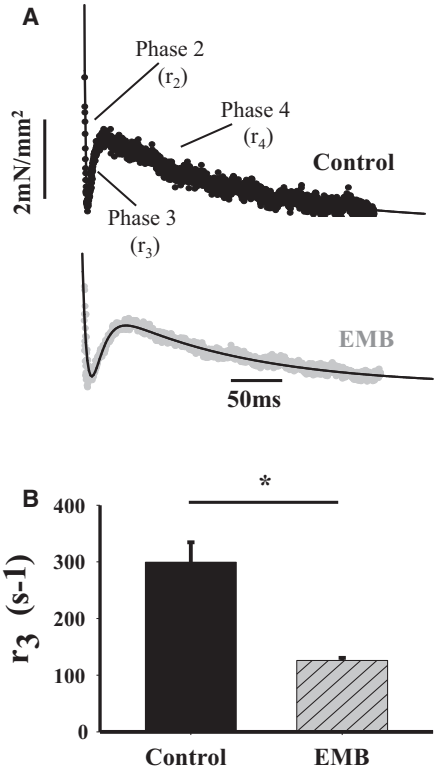

FIGURE 3 Stretch activation kinetics of EMB and control jump muscle fibers obtained at 8 mM Pi. (*A*) Individual stretch activation traces following a 1% ML step over 0.5 ms from control and EMB fibers were fitted to the sum of 3 exponential curves: $a_3[1\text{-}\exp(-r_3t)] + a_2\exp(-r_2t) + a_4\exp(-r_4t) +$ offset. Fitted line is shown in black. Rate of phase 2, r_2; rate of phase 3, r_3; rate of phase 4, r_4. (*B*) r_3 of control jump muscles decreased when EMB was expressed (*$P < 0.05$, Student's *t-test*).

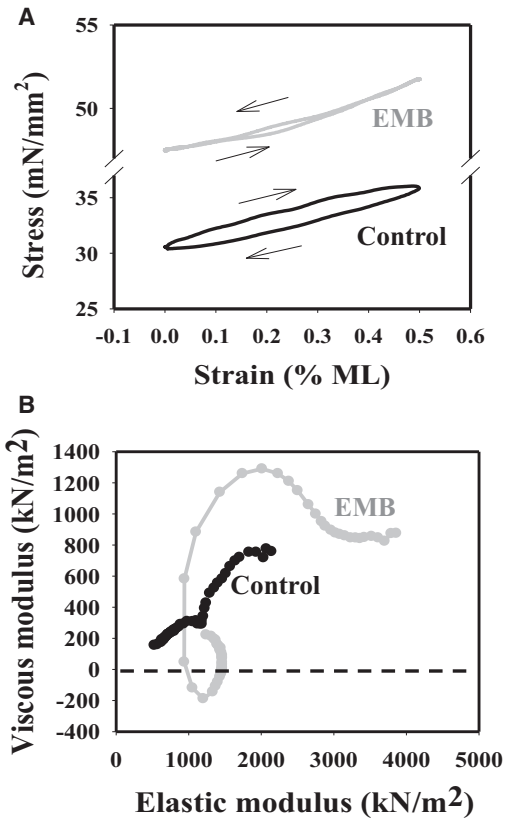

FIGURE 4 Representative (*A*) work loop and (*B*) nyquist plots of EMB and control jump muscle fibers obtained at 8 mM Pi. That EMB generates positive work and power is shown by both the counterclockwise EMB work loop trace and the EMB Nyquist plot dipping below zero.

Pi. Under all conditions tested, the jump muscle was unable to generate any positive work or power (Fig. 4). We tried a range of length changes (0.25–1% ML) and oscillation frequencies (1–60 Hz). The highest power production out of all the individual control fibers tested was −25.7 W/m^3. The optimal conditions that produced the most (least negative) power for control fibers were a peak-to-peak length oscillation of 0.5% strain amplitude of ML at 31.9 ± 5.2 Hz (Table 4). Under these conditions, control fibers produced clockwise work loops (Fig. 4 *A*), indicating they absorb work and power.

In contrast, fibers expressing the EMB isoform were capable of producing net positive work and power. The clockwise work loops of control fibers were transformed to be counter clockwise (Fig. 4 *A*). Compared to control fibers producing their maximum power, EMB fibers produced maximum power at a much lower frequency, but the same amount of length oscillation, 0.5% ML, was optimal (Table 4).

Sinusoidal analysis

To further test the ability of jump muscle fibers to generate oscillatory power at 8 mM Pi, we performed small amplitude sinusoidal analysis (0.125% ML). This tests a broader frequency range (0.5–500 Hz) than we could examine with the larger amplitude work loops as the larger amplitude loops slowly degrade the fiber, whereas small amplitudes

TABLE 3 Stretch activation kinetics of *Drosophila* jump muscles

	r_2 (s^{-1})	r_3 (s^{-1})a	r_4 (s^{-1})	*n*
Control	305.3 ± 36	299.4 ± 35.1	6.3 ± 0.8	11
EMB	134.1 ± 4.6[a]	126 ± 4.6[a]	7.3 ± 0.9	11

Values are mean ± SE; *n*, number of fibers; r_2, rate of phase 2, r_3, rate of phase 3, r_4, rate of phase 4 (see Fig. 1).
[a]$P < 0.05$, significantly different from control, Student's *t-test*. Measurements were made at pCa 5.0, 8 mM Pi and 15°C.

TABLE 4 Work and power generation by *Drosophila* jump muscles

	Work(nJ/mm3)	Power (W/m^3)	Frequency (Hz)	Strain (% ML)	*n*
Control	−4.0 ± 1.0	−87.8 ± 24.3	31.9 ± 5.2	0.5 ± 0.0	8
EMB	0.5 ± 0.5[a]	1.3 ± 1.6[a]	5.3 ± 0.6[a]	0.5 ± 0.0	10

Values are mean ± SE; *n*, number of fibers.
[a]$P < 0.05$, significantly different from control, Student's *t-test*. Measurements were made at 8 mM Pi using the work loop technique.

cause little to no degradation in performance. The shape of the Nyquist plots from control fibers is different than Nyquist plots from oscillatory muscles that can produce power at pCa 5.0 as it never dips below zero (Fig. 4 *B*). This shows that the control jump muscle fibers absorb work and produce negative power over the entire frequency range. EMB myosin changed the shape of jump muscle fibers' Nyquist plots to form a loop that dipped below zero, indicating EMB fibers produce positive work and power over a frequency range of 3–6 Hz. EMB fibers produced a maximum sinusoidal power of 2.1 ± 0.4 W/m^3 at 5.0 ± 0.6 Hz (see the Supporting Material, Table 1).

Phosphate effects on tension, stretch activation, and power generation

To explore the underlying mechanism of how EMB myosin increases SA of jump muscles, we observed the effects of 0, 8, and 16 mM Pi on isometric tension, F_{SA}, r_3, and power generation of control and EMB fibers (Fig. 5). F_O of both control and EMB fibers decreased when Pi was increased from 0 to 8 mM Pi (Fig. 5 *A*). Increasing Pi from 0 to 8 mm increased F_{SA} for EMB fibers. For control fibers, Pi had no effect on F_{SA} until 16 mM Pi where it slightly decreased F_{SA} (Fig. 5 *B*). Pi increased r_3 for both fiber types (Fig. 5 *C*). At 0 mM Pi, r_3 was not different between the two fiber types, but increasing Pi had more of an effect on control r_3 values such that at high Pi concentration, control fiber r_3 was much faster. The increase in EMB r_3 due to Pi appears to saturate at 8 mM Pi or earlier. Pi increased net power output of both control and EMB fibers as measured using the work loop assay (Fig. 5 *D*). However, control fibers were not able to generate any positive power at any Pi concentrations, whereas EMB fibers started to generate positive power around 4 mM Pi.

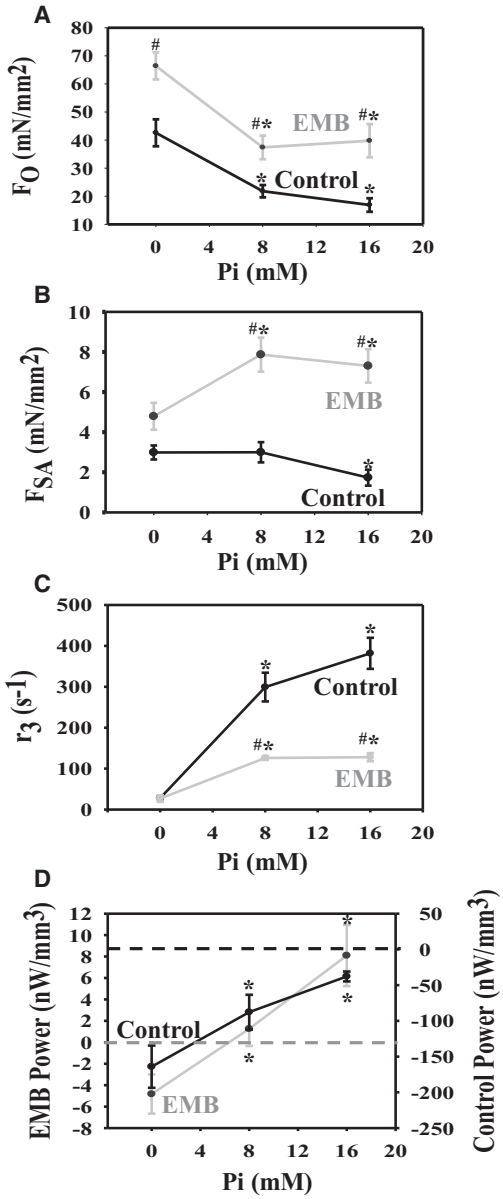

FIGURE 5 Influence of Pi on (*A*) isometric tension (F_O) (*B*) stretch activation tension (F_{SA}) (*C*) rate of SA force regeneration, r_3, and (*D*) power generation measured using the work loop technique of control and EMB fibers. Note the different *y*-axis scales. Dashed lines show 0 W/m^3 power for each set of fibers. *$P < 0.05$, Student's *t-test*, compared to 0 mM Pi; #$P < 0.05$, Student's *t-test*, compared to control fibers. *N* values for control and EMB averages are 10 and 11 for panel *A*, 10 and 16 for *B*, 11 and 11 for *C*, and 8 and 10 for *D*, respectively.

DISCUSSION

Stretch activation of skinned *Drosophila* jump muscles

Our *Drosophila* jump muscle preparation displayed the force characteristics of a minimally stretch-activated muscle type, showing only a 12% increase in tension relative to calcium-activated tension. This is similar to F_{SA} observed for most vertebrate skeletal muscle types (14), rather than the very prominent F_{SA} of its companion thorax muscle, the IFM. IFM F_{SA} is twofold higher than isometric tension (27). To measure jump muscle F_{SA}, we used our new method of paring down the entire jump muscle to a bundle of just 8–10 fibers (24). This contrasts with an entire skinned muscle preparation used in the only other mechanical study of isolated *Drosophila* jump muscle of which we are aware (22). Similar to our finding of a very minimal increase in tension due to SA, Peckham et al. found a 20% increase above calcium-activated isometric tension. The rates of force recovery (r_3) measured by the two jump muscle studies are also close in value. We measured 299 ± 35s^{-1} compared to 250 ± 32 s^{-1} for the entire muscle (22). The slight differences in F_{SA} and r_3 between our study and Peckham et al. are likely due to differences in cross-sectional area estimates and different activation solution components. The likely reason for the jump muscle not evolving significant F_{SA} is probably related to its functional

role of extending the center leg, a function most often used for jumping and initiating flight (20,21). The jump muscle is likely not lengthened before shortening to extend the leg, thus SA would not be beneficial.

An embryonic myosin isoform transforms jump muscles to be stretch activated

Our results show that specific MHC isoforms can enable significant gains in F_{SA} as we transformed the *Drosophila* jump muscle from a minimal to modest SA muscle type. The increase in F_{SA} could theoretically be due to a secondary effect of EMB expression. Perhaps EMB expression is upregulating expression of another isoform or causing a change in phosphorylation of another muscle protein isoform. Although we cannot rule out these possibilities, previous studies of EMB expression in IFM and jump muscles did not indicate any change in muscle protein expression based on protein gel profiles (23,24). We have also not seen any indication in any of our other experiments involving transgenic myosin expression (19).

Increased cyclical power generation can be used as a test to gauge if the F_{SA} increase is functionally significant. SA either enables power generation under constant calcium conditions, such as in IFM, or it increases power in a cycling calcium situation, such as in cardiac muscle. Using both sinusoidal and work loop analysis to measure power, we showed that EMB transforms the control jump muscle from being unable to generate work or power to positive work and power generation. The amount of positive work and power produced at 8 mm Pi indicates that the increase in F_{SA} is at least partially responsible for the increase in power (Supporting Material, Table 1). EMB produced 2.3-fold higher positive work (work during shortening) than control jump muscle. EMB negative work (work during lengthening) was also higher than control fiber negative work, but the difference was not as great as that seen with positive work.

The amount of work and power generation produced by jump muscle expressing EMB is similar to that produced by mouse heart muscle measured under comparable conditions (28). Mouse skinned myocardial strips produced 0.3 nJ/mm^3 of work at 8 Hz, which when multiplied is 2.4 W/m^3 power generation. This is similar to EMB's 0.5 nJ/mm^3 work and 1.3 W/m^3 power values (Table 4). Cardiac muscle power is enhanced by its SA properties (4). A recent study of skinned rat myocardium found that SA substantially increases force generation (15). This study also examined the influence of the two cardiac myosin isoforms on SA. No significant differences in F_{SA} between cardiac α and β myosin isoforms were found. This is the only other study of which we are aware that has directly compared the influence of myosin isoforms on F_{SA} when expressed in the same muscle type background.

Even when expressing EMB, the jump muscle does not produce as much power or F_{SA} as insect flight muscle. *Drosophil*a IFM generates ~100 W/m^3 as measured by sinusoidal analysis (29), and F_{SA} increases force generation twofold. This means that either the IFM myosin isoform enables more F_{SA} force than EMB, and/or another mechanism is operating in the IFM to significantly boost F_{SA} and power. Variation in more than one muscle protein is likely required for prominent SA as IFM has several protein isoform differences compared to other muscles in the fly (30). In particular, evidence is accumulating that a thin filament-based mechanism contributes to IFM SA (10,11). Thus, although our study shows that myosin isoforms can endow muscles with a moderate amount of SA, myosin is likely just one protein component out of several that must be modified to produce a highly SA muscle type.

In contrast to EMB's influence on F_{SA}, we were not surprised that EMB slowed SA kinetics. Many studies have shown that r_3 correlates with relative muscle shortening speed and/or myosin isoform in mammalian skeletal and cardiac muscles (1,4,13–15,31–33). We previously found that expressing EMB in the jump muscle decreased shortening velocity by 50% (24). Thus, the ~60% decrease in r_3 further validates that EMB has slower cross-bridge kinetics, in general, than the native jump muscle. Interestingly, the slower r_3 was only significant with added Pi (Fig. 5 *C*), suggesting that one difference in their cross-bridge cycles is different kinetics of the Pi release/rebinding step.

Influence of phosphate on stretch activation and power generation

Pi was not only required for a significant difference in r_3 between EMB and control jump muscle, but also for positive power generation. About 4 mM Pi was required for positive power generation, and power increased with increasing [Pi]. This correlated with the increase in F_{SA} seen in EMB fibers up to 8 mM Pi. Although the effect of Pi on F_{SA} stopped around 8 mM for EMB, power still increased (Fig. 5). Similarly, although no increase in F_{SA} was observed for control fibers with increasing [Pi], power still increased (became less negative) with Pi concentration. Thus, there is likely an additional reason for the increase in power. The decrease in force generation by Pi, which we observed in our study (Table 1 and Fig. 5 *A*) is well documented (34). Furthermore, a muscle property known as shortening deactivation causes a delayed decrease in force (3). If either shortening deactivation or Pi causes a decrease in force during lengthening then work during lengthening (negative work) will decrease and net work and power will increase. For both EMB and native jump muscle, positive work and negative work both decreased with increasing Pi concentrations. For jump muscle, we measured a 59% decrease in negative work compared to a 57% decrease for positive work over the 0 to 16 mM Pi range (Supporting Material, Table 1). In contrast, for EMB there was only a 38% loss of positive work compared to a 48% decrease in negative

work. Thus, for both isoforms, negative work is decreased more than positive work, leading to an increased power generation (or less negative power in the case of jump muscle). However, EMB lost less positive work, due to stronger F_{SA}, resulting in positive power (Fig. 5 *D*).

Stretch activation mechanism for the embryonic myosin isoform

Because positive power and a significant difference in F_{SA} between the isoforms was dependent on the presence of Pi, we propose that the most likely mechanism by which EMB increases F_{SA} is related to steps in the cross-bridge cycle involving Pi release and rebinding (Fig. 6). When an EMB expressing fiber is stretched (phase 1), the population of cross-bridges in weakly bound states is likely increased by stretch driving some of the strongly bound cross-bridges backward to the preceding weakly bound state (contributing to the phase 2 decline in force). Pi rebinding probably increases the probability of the backward step occurring that may involve reversal of the power stroke. The temporary increase in the number of cross-bridges in the weakly bound states increases the number of cross-bridges available to rapidly bind and generate force during phase 3 leading to more strongly bound cross-bridges than before the initial stretch. For the EMB myosin to generate greater F_{SA}, it must more easily be driven back to the prepower stroke state by stretch than wild-type, and/or stretch increases its affinity for Pi more than wild-type. Another factor contributing to greater F_{SA} may be a decrease in the forward detachment rate of strongly bound cross-bridges. However, our current study provides no insight into this possibility.

The idea of Pi driving cross-bridges back into the prestroke state from strongly bound states is well supported by many studies (34–40). This is the main explanation for how increasing Pi reduces calcium-activated isometric force. Recent studies also support the idea that stretch (strain on myosin) can cause cross-bridges to transition into the prepower stroke position (41–45). At least one study, which measured muscle Pi release rates during and following stretch, strongly suggests that stretch redistributes actomyosin cross-bridges to their Pi-containing state (46). The free energy for the reversal could come from the stretch itself as put forth by theoretical models such as that of Baker et al. (47).

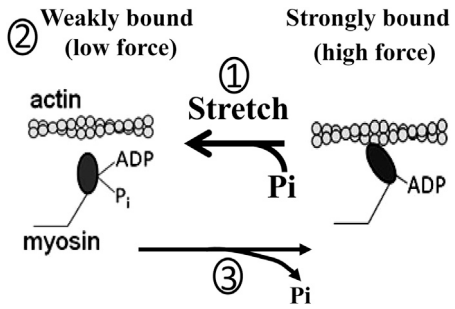

FIGURE 6 Hypothesis for SA myosin isoforms. Muscle stretch in the presence of Pi (1 = phase 1 in Fig. 1) drives some myosins back to a weakly bound state (contributing to phase 2). This adds to the pool of weakly bound myosins that can quickly transition into force-generating states, increasing the total number of myosins strongly bound during phase 3. For moderately SA myosins, such as EMB, to generate higher F_{SA}, they must more easily be driven back to the prepower stroke state by stretch than wild-type and/or stretch increases their affinity for Pi.

Structural basis for the embryonic myosin increasing stretch activation force

Drosophila myosin's expression mechanism guides us to regions that must be responsible for functional differences. *Drosophila* MHC is encoded by a single *Mhc* gene, which produces MHC isoforms by alternative splicing of five alternative exons (3,7,9,11,15) (16,17,48,49). The EMB and jump muscle myosins differ at all five alternative exons. We have shown that alternative exons 3, 7, 9, 11, and 15 influence various mechanical properties of IFM fibers by exchanging the corresponding exon regions between IFM and EMB myosins and measuring how this influences IFM mechanical properties (29,50–54). Our previous experiments suggest exon 9, which encodes the relay loop of the myosin head, is critical in intramolecular transmission of strain/stress information (55). The relay helix structurally links the active site to the lever arm by physically contacting the converter at one end and transitioning into the switch 2 motif at the other end. Switch 2 interacts with the terminal Pi of MgATP during the cross-bridge cycle (56). Thus, we propose that the relay is the most likely structural region for modifying F_{SA}.

SUPPORTING MATERIAL

One table is available at http://www.biophysj.org/biophysj/supplemental/S0006-3495(13)00582-1.

We thank Bernadette Glasheen for excellent technical assistance.

Financial support was provided by NIH NIAMS grant AR055611 (to D.M.S.) and American Heart Association Predoctoral Fellowship 11PRE5630000 (to C.Z.).

REFERENCES

1. Steiger, G. J. 1977. Stretch activation and tension transients in cardiac, skeletal and insect flight muscle. *In* Insect Flight Muscle. R. T. Tregear, editor. North Holland, Amsterdam. 221–268.
2. Pringle, J. W. S. 1978. The Croonian Lecture, 1977. Stretch activation of muscle: function and mechanism. *Proc. R. Soc. Lond. B Biol. Sci.* 201:107–130.
3. Josephson, R. K., J. G. Malamud, and D. R. Stokes. 2000. Asynchronous muscle: a primer. *J. Exp. Biol.* 203:2713–2722.
4. Steiger, G. J. 1971. Stretch activation and myogenic oscillation of isolated contractile structures of heart muscle. *Pflugers Arch.* 330:347–361.

5. Wray, J. S. 1979. Filament geometry and the activation of insect flight muscles. *Nature.* 280:325–326.
6. Granzier, H. L. M., and K. Wang. 1993. Interplay between passive tension and strong and weak binding cross-bridges in insect indirect flight muscle. A functional dissection by gelsolin-mediated thin filament removal. *J. Gen. Physiol.* 101:235–270.
7. Fukuda, N., and H. L. Granzier. 2005. Titin/connectin-based modulation of the Frank-Starling mechanism of the heart. *J. Muscle Res. Cell Motil.* 26:319–323.
8. Tohtong, R., H. Yamashita, …, D. Maughan. 1995. Impairment of muscle function caused by mutations of phosphorylation sites in myosin regulatory light chain. *Nature.* 374:650–653.
9. Dickinson, M. H., C. J. Hyatt, …, D. W. Maughan. 1997. Phosphorylation-dependent power output of transgenic flies: an integrated study. *Biophys. J.* 73:3122–3134.
10. Perz-Edwards, R. J., T. C. Irving, …, M. K. Reedy. 2011. X-ray diffraction evidence for myosin-troponin connections and tropomyosin movement during stretch activation of insect flight muscle. *Proc. Natl. Acad. Sci. USA.* 108:120–125.
11. Bullard, B., and A. Pastore. 2011. Regulating the contraction of insect flight muscle. *J. Muscle Res. Cell Motil.* 32:303–313.
12. Thorson, J., and D. C. S. White. 1983. Role of cross-bridge distortion in the small- signal mechanical dynamics of insect and rabbit skeletal muscle. *J. Physiol. (Great Britain).* 343:59–84.
13. Galler, S., T. L. Schmitt, and D. Pette. 1994. Stretch activation, unloaded shortening velocity, and myosin heavy chain isoforms of rat skeletal muscle fibres. *J. Physiol.* 478:513–521.
14. Galler, S., K. Hilber, and D. Pette. 1997. Stretch activation and myosin heavy chain isoforms of rat, rabbit and human skeletal muscle fibres. *J. Muscle Res. Cell Motil.* 18:441–448.
15. Stelzer, J. E., S. L. Brickson, …, R. L. Moss. 2007. Role of myosin heavy chain composition in the stretch activation response of rat myocardium. *J. Physiol.* 579:161–173.
16. Rozek, C. E., and N. Davidson. 1983. *Drosophila* has one myosin heavy-chain gene with three developmentally regulated transcripts. *Cell.* 32:23–34.
17. Bernstein, S. I., K. Mogami, …, C. P. Emerson, Jr. 1983. *Drosophila* muscle myosin heavy chain encoded by a single gene in a cluster of muscle mutations. *Nature.* 302:393–397.
18. Swank, D. M., A. F. Knowles, …, S. I. Bernstein. 2000. The converter domain of myosin influences actin velocity and ATPase rate: an integrative analysis of the *Drosophila* exon 11 region. *Biophys. J.* 78:244A.
19. Swank, D. M. 2012. Mechanical analysis of *Drosophila* indirect flight and jump muscles. *Methods.* 56:69–77.
20. Zumstein, N., O. Forman, …, C. J. Elliott. 2004. Distance and force production during jumping in wild-type and mutant *Drosophila* melanogaster. *J. Exp. Biol.* 207:3515–3522.
21. Card, G., and M. Dickinson. 2008. Performance trade-offs in the flight initiation of *Drosophila*. *J. Exp. Biol.* 211:341–353.
22. Peckham, M., J. E. Molloy, …, D. C. White. 1990. Physiological properties of the dorsal longitudinal flight muscle and the tergal depressor of the trochanter muscle of *Drosophila melanogaster. J. Muscle Res. Cell Motil.* 11:203–215.
23. Wells, L., K. A. Edwards, and S. I. Bernstein. 1996. Myosin heavy chain isoforms regulate muscle function but not myofibril assembly. *EMBO J.* 15:4454–4459.
24. Eldred, C. C., D. R. Simeonov, …, D. M. Swank. 2010. The mechanical properties of *Drosophila* jump muscle expressing wild-type and embryonic Myosin isoforms. *Biophys. J.* 98:1218–1226.
25. Huxley, A. F., and R. M. Simmons. 1971. Mechanical properties of the cross-bridges of frog striated muscle. *J. Physiol.* 218 (*Suppl*):59P–60P.
26. Yang, C., C. N. Kaplan, …, D. M. Swank. 2010. The influence of myosin converter and relay domains on cross-bridge kinetics of *Drosophila* indirect flight muscle. *Biophys. J.* 99:1546–1555.
27. Wang, Q., C. Zhao, and D. M. Swank. 2011. Calcium and stretch activation modulate power generation in *Drosophila* flight muscle. *Biophys. J.* 101:2207–2213.
28. Palmer, B. M., T. Noguchi, …, M. M. LeWinter. 2004. Effect of cardiac myosin binding protein-C on mechanoenergetics in mouse myocardium. *Circ. Res.* 94:1615–1622.
29. Swank, D. M., A. F. Knowles, …, S. I. Bernstein. 2002. The myosin converter domain modulates muscle performance. *Nat. Cell Biol.* 4:312–316.
30. Maughan, D., and J. Vigoreaux. 2005. Nature's strategy for optimizing power generation in insect flight muscle. *Adv. Exp. Med. Biol.* 565:157–166, discussion 167, 371–157.
31. Galler, S., T. L. Schmitt, …, D. Pette. 1997. Stretch activation and isoforms of myosin heavy chain and troponin-T of rat skeletal muscle fibres. *J. Muscle Res. Cell Motil.* 18:555–561.
32. Andruchova, O., G. M. Stephenson, …, S. Galler. 2006. Myosin heavy chain isoform composition and stretch activation kinetics in single fibres of *Xenopus laevis* iliofibularis muscle. *J. Physiol.* 574:307–317.
33. Galler, S., E. Puchert, …, D. Pette. 2002. Kinetic properties of cardiac myosin heavy chain isoforms in rat. *Pflugers Arch.* 445:218–223.
34. Hibberd, M. G., J. A. Dantzig, …, Y. E. Goldman. 1985. Phosphate release and force generation in skeletal muscle fibers. *Science.* 228:1317–1319.
35. Rüegg, J. C., M. Schädler, …, G. Müller. 1971. Effects of inorganic phosphate on the contractile mechanism. *Pflugers Arch.* 325:359–364.
36. Kawai, M., K. Güth, …, J. C. Rüegg. 1987. The effect of inorganic phosphate on the ATP hydrolysis rate and the tension transients in chemically skinned rabbit psoas fibers. *Pflugers Arch.* 408:1–9.
37. Pate, E., and R. Cooke. 1989. Addition of phosphate to active muscle fibers probes actomyosin states within the powerstroke. *Pflugers Arch.* 414:73–81.
38. Cooke, R., K. Franks, …, E. Pate. 1988. The inhibition of rabbit skeletal muscle contraction by hydrogen ions and phosphate. *J. Physiol.* 395:77–97.
39. Millar, N. C., and E. Homsher. 1990. The effect of phosphate and calcium on force generation in glycerinated rabbit skeletal muscle fibers. A steady-state and transient kinetic study. *J. Biol. Chem.* 265:20234–20240.
40. Dantzig, J. A., Y. E. Goldman, …, E. Homsher. 1992. Reversal of the cross-bridge force-generating transition by photogeneration of phosphate in rabbit psoas muscle fibres. *J. Physiol.* 451:247–278.
41. Lombardi, V., and G. Piazzesi. 1990. The contractile response during steady lengthening of stimulated frog muscle fibres. *J. Physiol.* 431:141–171.
42. Wang, G., and M. Kawai. 2001. Effect of temperature on elementary steps of the cross-bridge cycle in rabbit soleus slow-twitch muscle fibres. *J. Physiol.* 531:219–234.
43. Piazzesi, G., M. Reconditi, …, V. Lombardi. 2003. Temperature dependence of the force-generating process in single fibres from frog skeletal muscle. *J. Physiol.* 549:93–106.
44. Colombini, B., M. Nocella, …, M. A. Bagni. 2007. Cross-bridge properties during force enhancement by slow stretching in single intact frog muscle fibres. *J. Physiol.* 585:607–615.
45. Colombini, B., M. Nocella, …, M. A. Bagni. 2008. Effect of temperature on cross-bridge properties in intact frog muscle fibers. *Am. J. Physiol. Cell Physiol.* 294:C1113–C1117.
46. Mansfield, C., T. G. West, …, M. A. Ferenczi. 2012. Stretch of contracting cardiac muscle abruptly decreases the rate of phosphate release at high and low calcium. *J. Biol. Chem.* 287:25696–25705.
47. Baker, J. E. 2004. Free energy transduction in a chemical motor model. *J. Theor. Biol.* 228:467–476.
48. Zhang, S., and S. I. Bernstein. 2001. Spatially and temporally regulated expression of myosin heavy chain alternative exons during *Drosophila* embryogenesis. *Mech. Dev.* 101:35–45.

49. Bernstein, S. I., C. J. Hansen, …, C. P. Emerson, Jr. 1986. Alternative RNA splicing generates transcripts encoding a thorax-specific isoform of *Drosophila melanogaster* myosin heavy chain. *Mol. Cell. Biol.* 6:2511–2519.

50. Swank, D. M., A. F. Knowles, …, S. I. Bernstein. 2003. Variable N-terminal regions of muscle myosin heavy chain modulate ATPase rate and actin sliding velocity. *J. Biol. Chem.* 278:17475–17482.

51. Littlefield, K. P., D. M. Swank, …, S. I. Bernstein. 2003. The converter domain modulates kinetic properties of *Drosophila* myosin. *Am. J. Physiol. Cell Physiol.* 284:C1031–C1038.

52. Swank, D. M., W. A. Kronert, …, D. W. Maughan. 2004. Alternative N-terminal regions of *Drosophila* myosin heavy chain tune muscle kinetics for optimal power output. *Biophys. J.* 87:1805–1814.

53. Swank, D. M., J. Braddock, …, D. W. Maughan. 2006. An alternative domain near the ATP binding pocket of *Drosophila* myosin affects muscle fiber kinetics. *Biophys. J.* 90:2427–2435.

54. Swank, D. M., V. K. Vishnudas, and D. W. Maughan. 2006. An exceptionally fast actomyosin reaction powers insect flight muscle. *Proc. Natl. Acad. Sci. USA.* 103:17543–17547.

55. Yang, C., S. Ramanath, …, D. M. Swank. 2008. Alternative versions of the myosin relay domain differentially respond to load to influence *Drosophila* muscle kinetics. *Biophys. J.* 95:5228–5237.

56. Trivedi, D. V., C. David, …, C. M. Yengo. 2012. Switch II mutants reveal coupling between the nucleotide- and actin-binding regions in myosin V. *Biophys. J.* 102:2545–2555.